

AdvART: Adversarial Art for Camouflaged Object Detection Attacks

Amira Guesmi¹, Ioan Marius Bilasco², Muhammad Shafique¹, and Ihcen Alouani³

¹*eBrain Lab, Division of Engineering, New York University (NYU) Abu Dhabi, UAE*

²*CRISAL, Univ. Lille, CNRS, Centrale Lille, UMR 9189, France*

³*CSIT, Queen's University Belfast, UK*

Abstract—Physical adversarial attacks pose a significant practical threat as it deceives deep learning systems operating in the real world by producing prominent and maliciously designed physical perturbations. Emphasizing the evaluation of naturalness is crucial in such attacks, as humans can readily detect and eliminate unnatural manipulations. To overcome this limitation, recent work has proposed leveraging generative adversarial networks (GANs) to generate naturalistic patches, which may not catch human's attention. However, these approaches suffer from a limited latent space which leads to an inevitable trade-off between naturalness and attack efficiency. In this paper, we propose a novel approach to generate naturalistic and inconspicuous adversarial patches. Specifically, we redefine the optimization problem by introducing an additional loss term to the cost function. This term works as a semantic constraint to ensure that the generated camouflage pattern holds semantic meaning rather than arbitrary patterns. The additional term leverages similarity metrics to construct a similarity loss that we optimize within the global objective function. Our technique is based on directly manipulating the pixel values in the patch, which gives higher flexibility and larger space compared to the GAN-based techniques that are based on indirectly optimizing the patch by modifying the latent vector. Our attack achieves superior success rate of up to 91.19% and 72%, respectively, in the digital world and when deployed in smart cameras at the edge compared to the GAN-based technique.

I. INTRODUCTION

Physical attack scenarios [1]–[4] involve attackers designing printable adversarial patches for deployment in scenes captured by the victim model. These patches are not generated with constraints on noise magnitude, but rather on location and printability. Considering their practical application in real-world situations, physical patch-based attacks are more damaging and practical for real-life scenarios. This paper focuses on adversarial patches and specifically investigates their undetectability from a naturalistic distribution perspective.

Prior research on adversarial patches for object detection [5]–[8] has primarily focused on enhancing attack performance and increasing the strength of adversarial noise. However, this approach often leads to the creation of conspicuous and noticeable patches that can be easily identified by human observers. To tackle this issue, some researchers have proposed the utilization of generative adversarial networks (GANs) [9]–[12] to generate naturalistic adversarial patches. However, these methods were proven to suffer from an extremely limited latent space [11], [13], which limits the performance of the

generated patch especially when trying to incorporate multiple transformations in the optimization process. In addition, the generation of a naturalistic pattern is not always guaranteed. As shown in Figure 1, with different initialization the GAN-based framework converges to unrealistic patterns.

To overcome this limitation and to generate effective attacks with naturalistic patterns, we propose a novel framework (AdvART). Our approach involves optimizing towards a target natural image while simultaneously maximizing the loss of the victim model, aimed to undermine detection systems. This approach involves an optimization process utilizing a novel objective function that incorporates a semantic constraint to guide the pattern of the generated noise and converge to a semantically meaningful adversarial pattern.

Novel contributions – The main contributions of this paper are summarized as follows:

- We propose a novel framework (AdvART) that generates naturalistic patches while retaining attack performance. Our technique incorporates a semantic constraint to force the optimized noise to follow a predefined natural/artistic pattern.
- Our proposed technique offers greater flexibility compared to GAN-based techniques, allowing for the incorporation of multiple transformations. These transformations are strategically aimed at enhancing the overall robustness of the generated patch.
- We conduct a comprehensive analysis of the effectiveness of the proposed approach by evaluating its performance and attack success rate in terms of mean average precision (mAP), as well as examining the patch's transferability across different detectors. Our patch achieves a mAP of 8.81%, 34.93%, 17.7%, and 15.82% in the digital world (INRIA dataset [14]) when targeting the YOLOv4tiny, YOLOv3tiny, YOLOv4 [15], and YOLOv3 [16] detectors, respectively for edge systems.
- We demonstrate the effectiveness of our proposed patch in real-world scenarios, achieving a success rate of 72%.

II. RELATED WORK

At first, the proposed physical attacks aiming at fooling person detectors were generated without any constraints on the patch appearance [7], [18]–[20]. Their main focus was on performance and producing effective attacks without any focus on attack stealthiness. To overcome this limitation, some works

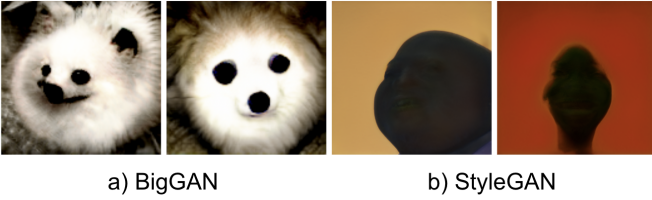


Fig. 1: Different results of different attempts to generate NAP patches [11] using different latent vector initialization for different GANs: a) BigGAN, and b) StyleGAN.

proposed to leverage the learned image manifold of pre-trained Generative Adversarial Networks (GANs) upon real-world images. Authors in [11] proposed a naturalistic patch (NAP) based on two GANs (i.e., BigGAN [21] and StyleGAN [22]). The training on GANs needs a lot of resources in terms of computing units and time to converge if they converge to realistic images in the first place. Authors in [17] also proposed a universal camouflage pattern (UPC) that is visually similar to natural images. In [9], authors tried to extend the existing work to make the patch suppress objects near the patch. However, what they proposed is unrealistic in terms of the positioning of the patch and its size. Also, another limitation of these approaches is that the patch will be restricted to objects that the GAN was trained to produce, these approaches may not always converge to a natural looking patch. A comparison of AdvART with state-of-the-art attacks is provided in Table I. In Figure 2, we illustrate different state of the art adversarial patches in addition to ours (AdvART-based).

TABLE I: AdvART vs State-of-the-Art adversarial patches. (EOT: Expectation Over Transformations, TV: Total Variation, NPS: Non-Printability Score).

Attack	Robustness	Stealthiness	Form
AdvYOLO [7]	EOT, TV, NPS	(-)	Cardboard
UPC [17]	EOT, TV	L_∞ norm	Clothing
NAP [11]	TV	GAN	Clothing
AdvART (ours)	EOT, TV	L_{sim}	Clothing

III. ADVART: OUR ADVERSARIAL ART FRAMEWORK FOR OBJECT DETECTION ATTACKS

A. Problem formulation

In an object detection context, given a benign image I , the purpose of the adversarial attack is to jeopardize the object detector and suppress the target objects using the maliciously designed adversarial example I^* . Technically, the adversarial example with a generated patch can be formulated as:

$$I^* = (1 - M_P) \odot I + M_P \odot P \quad (1)$$

\odot is the component-wise multiplication, P is the adversarial patch, and M_P is the patch mask, used to constrict the size, shape, and location of the adversarial patch. The problem of generating an adversarial example can be formulated as a

constrained optimization 2, given an original input image I and an object detector $F(\cdot)$:

$$\min_P \|P\|_p \text{ s.t. } F((1 - M_P) \odot I + M_P \odot P) \neq F(I) \quad (2)$$

The objective is to find a minimal adversarial noise, P , such that when placed on an arbitrary object from a target input domain U , it will selectively jeopardize the underlying DNN-based model $F(\cdot)$ by making objects undetectable. Note that one cannot find a closed-form solution for this optimization problem since the DNN-based model $F(\cdot)$ is a non-convex machine learning model. Therefore, Equation 2 can be formulated as follows to numerically solve the problem using empirical approximation techniques:

$$\arg \max_P \sum_{I \in U} l(F((1 - M_P) \odot I + M_P \odot P), F(I)) \quad (3)$$

where l is a predefined loss function. We can use existing optimization techniques (e.g., Adam [23]) to solve this problem. In each iteration of the training, the optimizer updates the adversarial patch P .

B. Overview of Our Framework

The primary objective of our research is to generate physical adversarial patches that effectively deceive DNN-based object detectors, without being conspicuous or attention-grabbing while being robust to real-world constraints. In this study, we place our focus on simultaneously fulfilling three essential requirements crucial for real-world applicability. These requirements are as follows:

- **Patch effectiveness:** Ensuring the generated patch significantly degrades the performance of the detector.
- **Patch stealthiness:** Ensuring that the patch remains inconspicuous to human observers and does not attract attention.
- **Patch robustness:** Maintaining the patch's attack capability in dynamic environments, including resilience to physical constraints.

To achieve these goals, we propose an objective function that incorporates a semantic constraint (i.e., similarity loss), which guarantees the artistic pattern of the adversarial patch. Additionally, a detection loss is employed to maintain the attack's performance while considering complex physical factors such as object size, shape, and location.

Figure 3 provides an overview of the proposed framework. Our aim is to optimize the adversarial patch P in such a way that the target object becomes undetectable by an object detector, while ensuring the patch retains a naturalistic and artistic pattern guided by a given benign image.

To achieve this, we employ several steps. Firstly, we pass the patch through a patch transformer, applying geometric transformations to enhance its robustness. Next, we overlay the patch onto the input image using generated masks. The resulting adversarial image is then fed into the object detector to compute the detection loss, similarity loss, and total variation.

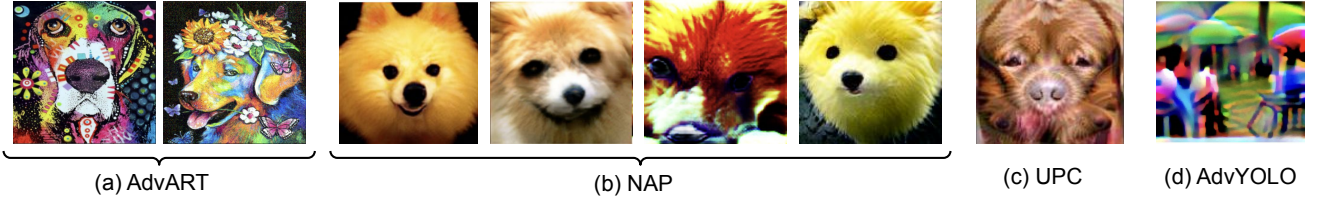


Fig. 2: AdvART patch vs State-of-the-Art patches: (a) AdvART patch, (b) NAP [11], (c) UPC patch [17], and (d) AdvYOLO [7].

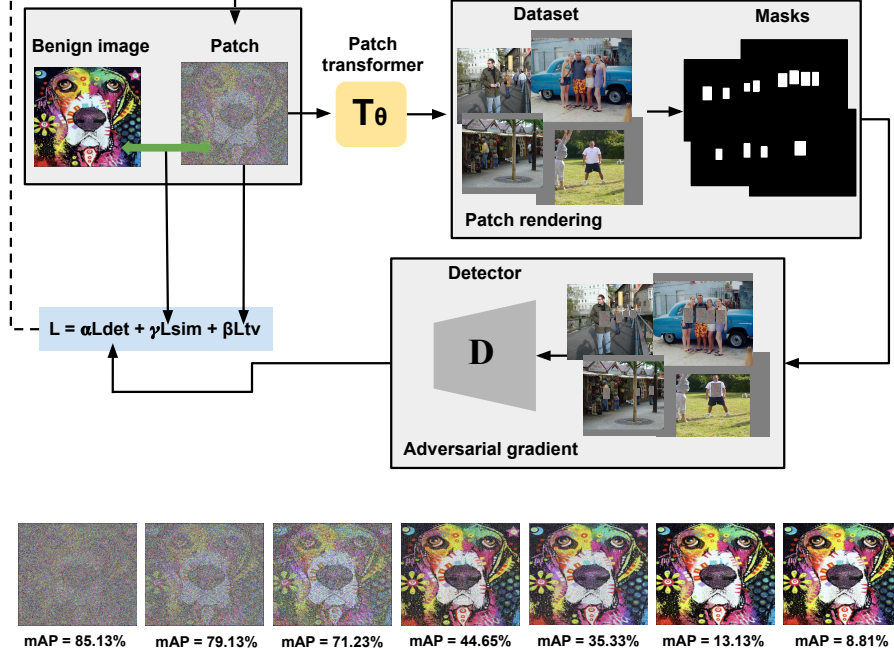


Fig. 3: Upper: Overview of the proposed framework: Bottom: Evolution of patch's appearance with the corresponding achieved mean average precision.

Using the gradient information obtained from the patch, we update the patch P . Our goal is to generate physical adversarial patches that possess a natural appearance while maintaining their effectiveness in evading detection. This is achieved through iterative gradient updates performed on the adversarial patch (P) in the pixel space, optimizing our objective defined as follows:

$$Loss_{total} = \alpha L_{det} + \beta L_{sim}^2 + \gamma L_{tv} \quad (4)$$

Where L_{det} is the adversarial detection loss (See Section III-C). L_{sim} is the similarity loss (See Section III-D). L_{tv} is the total variation loss on the generated image to encourage smoothness (See Section III-E). α , β , and γ are hyper-parameters used to scale the three losses. For our experiments we set $\alpha = 1$, $\beta = 8$, and $\gamma = 0.5$. We optimize the total loss using Adam [23] optimizer. We try to minimize the object function L_{total} and optimize the adversarial patch. We freeze all weights and biases in the object detector, and only update the pixel values of the adversarial patch.

C. Patch effectiveness

Object detectors like YOLO [15], [16], [24], [25] produce multiple boxes or detections. Our objective is to target two specific quantities for each detection j : the objectness probability D_{obj}^j and the class probability D_{cls}^j . By minimizing the objectness probability D_{obj}^j , we aim to prevent the j -th object from being detected altogether. Conversely, minimizing the class probability D_{cls}^j results in the j -th object being misclassified into a different class, such as a person being classified as a dog. In this paper, our focus is on targeting the person class. Therefore, we minimize both the objectness D_{obj}^j and class probabilities D_{cls}^j specifically for the person class. To speed up the iterations, we do not compute the loss over all detected boxes. Instead, we only consider the detected box with the highest objectness and class probabilities. Our adversarial detection loss is defined below:

$$L_{det} = \frac{1}{N} \sum_{i=1}^N \max_j [D_{obj}^j(I'_i) D_{cls}^j(I'_i)] \quad (5)$$

D. Patch Stealthiness

To ensure that the generated patch exhibits a pattern similar to a predefined natural or artistic pattern, we impose a constraint on its appearance. This is achieved through the use of a semantic constraint, where we select a natural/artistic image denoted as N , and we force the adversarial noise to follow the artistic pattern rather than having meaningless patterns and ensure that the generated camouflage pattern holds semantic meaning. The primary concept behind achieving a patch similar to an existing piece of art involves introducing a new loss term. This loss term quantifies the distance between the patch and the art piece, aiming to minimize this distance. Referred to as the similarity loss, it is specifically designed to reduce the disparity between the patch and a benign artistic image. By integrating this loss term, we facilitate the generation of a patch that closely resembles the artistic pattern. As depicted in Figure 3, which illustrates the changes in patch appearance during training and its corresponding impact on object detector performance in terms of mean average precision, naturalness is improved in conjunction with attack efficiency.

L_{sim} is the similarity loss between the target natural image N and the adversarial patch P . It is defined as:

MSE-based similarity loss

$$L_{sim} = \frac{1}{n} \sum_{i,j} (P_{i,j} - N_{i,j})^2 \quad (6)$$

Cosine similarity-based similarity loss

$$L_{sim} = - \left(\frac{\sum_{i,j} P_{i,j} N_{i,j}}{\sqrt{\sum_{i,j} P_{i,j}^2} \sqrt{\sum_{i,j} N_{i,j}^2}} \right) \quad (7)$$

We square the similarity loss term, to slow the rate of increase (the slope or the rate of change) and delay the convergence of the similarity metric with respect to the detection loss.

E. Patch Robustness

1) *Expectation Over Transformation (EOT)* [26]: We incorporate the physical world variables throughout the adversarial patch optimization process to increase its robustness and retain the same performance in realistic scenarios. Various factors, such as fluctuating lighting, various viewpoints, noise, etc., are frequently present in real-world scenarios. We use several physical transformations to simulate these dynamic factors. Technically, we take into account the transformations of the inclusion of variable conditions, such as adding noise, random rotation, variable scales, lighting variation, etc. The above physical transformation operations are performed using the patch transformer. The geometric transformations applied are: **Random scaling** of the patch to a size that is roughly equivalent to its physical size in the scene. Perform **random rotations** ($\pm 20^\circ$) on the patch P about the center of the bounding boxes $B_{i,k}^U$. The above simulate placement and printing size uncertainties. The color

space transformations are done by changing the pixel intensity values by adding **random noise** (± 0.1), performing **random contrast** adjustment of the value ($[0.8, 1.2]$), and **random brightness** adjustment (± 0.1). The resulting image $T_\theta(I_i)$ is forward propagated through the Object Detector.

2) *Total Variation Norm (TV loss)*: The characteristics of natural images include smooth and consistent patches with gradual color changes within each patch [27]. Therefore, to increase the plausibility of physical attacks, smooth and consistent perturbations are preferred. To address this issue, the total variation (TV) [27] loss is introduced to maintain the smoothness of the perturbation. For a perturbation P , TV loss is defined as:

$$L_{tv} = \sum_{i,j} \sqrt{(P_{i+1,j} - P_{i,j})^2 + (P_{i,j+1} - P_{i,j})^2} \quad (8)$$

Where the subindices i and j refer to the pixel coordinate of the patch P .

IV. EVALUATION OF ATTACK PERFORMANCE

TABLE II: Transferability analysis in terms of mAP of AdvART on INRIA dataset using different detectors.

Models	Yolov3	Yolov3tiny	Yolov4	Yolov4tiny
Yolov3 [16]	15.82%	52.77%	29.37%	58.24%
Yolov3tiny	41.46%	34.93%	37.46%	56.29%
Yolov4 [15]	27.18 %	41.36%	17.7%	65.84%
Yolov4tiny	60.70%	57.40%	47.46 %	8.81%

We use the mean average precision (mAP) as our evaluation metric. Same as in [7], [11], we use each detector's detection boxes on the clean dataset as the ground truth boxes (i.e., if there is no adversarial patch, the mAP of detectors will be 100%) and we report the mean average precision (mAP) when adding the adversarial patches. Table II shows the evaluation results on the INRIA dataset. We use four different detectors to generate the patches. The horizontal detectors are the victim ones and the verticals are the ones used for patch generation.

As shown in Table II, expectedly, when the victim detector used for training is the same one used for testing, we accomplish a great attack performance. Importantly, Table II shows that our patch is significantly transferable to other models.

TABLE III: Attack performance in terms of mAP of AdvART vs state-of-the-art adversarial patches.

Models	AdvART	NAP [11]	AdvYOLO [7]	UPC [17]
Yolov2	20.8%	12.06%	2.13%	48.62%
Yolov3	15.82%	34.93 %	22.51%	54.40%
Yolov3tiny	34.93%	10.02%	8.74%	63.82%
Yolov4	17.7 %	22.63%	12.89%	64.21 %
Yolov4tiny	8.81%	8.67%	3.25%	57.93 %

As shown in Table III, when we compare our technique to others, we can notice that some previously proposed methods

exhibit superior performance for some of the detectors. It's important to note that the reported results for the AdvYOLO [7] attack there were no constraint on the appearance of the patch which gave higher flexibility to attain higher attack performance. Additionally, the NAP [11] technique pertain to a specific scenario where the patch was trained without any transformations and tested without applying any transformations. However, it's crucial to emphasize that, as discussed in Section VII-B, when we train their patch with transformations with the aim of improving robustness, there is a noticeable decrease in patch performance. This phenomenon is observed in other techniques as well. Conversely, the results we report for our patch reflect a scenario where the patch is trained to accommodate various transformations. In this context, our patch undergoes training with the explicit inclusion of transformations, which is an essential factor contributing to its performance characteristics.

A. Cross-Dataset Evaluation


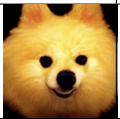


We use YOLOv4tiny to train an adversarial patch on the INRIA dataset and test the produced patch on the MPII dataset. As shown in Table IV, our patch is transferable cross-datasets. An adversarial patch generated on the INRIA dataset is still effective on MPII [28] with an mAP equal to 15.53%.

TABLE IV: Attack performance (mAP) of AdvART on MPII.

Datasets	INRIA	MPII
mAP	8.81%	15.53 %

V. SUBJECTIVE EVALUATION FOR THE NATURALNESS OF DIFFERENT ADVERSARIAL PATCHES

TABLE V: Subjective test for the naturalness evaluation of our adversarial patch with other baselines. The Naturalness scores are the average of percentages for each patch image over the whole group of participants.

Patches	AdvART	NAP [11]	UPC [17]	AdvYOLO [7]
Images				
Scores	94.45%	47.75%	18.15%	15%

Our proposed framework places a primary emphasis on the naturalness and inconspicuousness of the generated adversarial patch as perceived by human observers. To rigorously assess this aspect, we conducted a formal set of subjective evaluations, comparing the naturalness of our proposed patches against both baseline and real images. This subjective survey involved a diverse cohort of 20 participants, encompassing individuals of varied backgrounds, both male and female, aged between 19 and 59, and with no prior exposure to the topic. This comprehensive framework was taken to minimize potential biases and bolster the trustworthiness of our subjective evaluation.

Participants were tasked with providing a numerical score, ranging from 0 to 100%, to gauge both the naturalness and the absence of conspicuous patterns in the presented images. As presented in Table V, our patch received the highest score (94.45%) compared to NAP (47.75%). This outcome underscores the patch's capacity to seamlessly integrate with its surroundings or context, as assessed by the participants.

VI. PHYSICAL ATTACK EVALUATIONS

TABLE VI: Attack Success Rate (ASR) in Benign scenarios and when using AdvART and NAP [11] when attacking YOLOv4tiny.

	Benign	NAP	AdvART
Attack Success Rate	100%	55%	72%

We assessed the performance of our AdvART in real-world scenarios through the following setting: when the adversarial patch is printed on a t-shirt. By conducting evaluations in this physical context, we aimed to comprehensively evaluate the effectiveness of our technique. We run a physical attack evaluation by taking pictures of one person wearing the adversarial t-shirt (see Figure 4). We used YOLOv4tiny as the evaluation detector. Table VI reports the detection recall in the physical world and when our AdvART is printed on a t-shirt, only 28% of the time a person is detected.

VII. DISCUSSION

A. Influence of Different Similarity Metrics

We tested two different similarity metrics MSE and Cosine similarity used to measure the distance between two images to build our semantic constraint. As shown in Figure 5, when using the cosine similarity the optimization function converged faster to a more efficient patch (i.e., lower mAP). The MSE-based achieved an mAP of 14% however the cosine similarity based achieved a lower mAP of 8.81%. In Table VII, the Structural Similarity Index (SSIM) [29] was computed between the benign target artistic pattern and the generated patch, utilizing both the Cosine similarity and MSE. This evaluation allowed us to assess the level of structural similarity between the original pattern and the generated adversarial patch, considering both their visual resemblance and semantic consistency. The final patch generated using the cosine similarity is more realistic and closer to the target benign pattern with an SSIM score of 0.95 compared to 0.88 for MSE based similarity loss.

TABLE VII: SSIM between the benign target artistic pattern and the generated patch using Cosine similarity and MSE-based semantic constraint.

Similarity metric	Cosine Similarity	MSE
SSIM	0.95	0.88



Fig. 4: Illustrations of AdvART patch performance when printed on a t-shirt for different view angles.

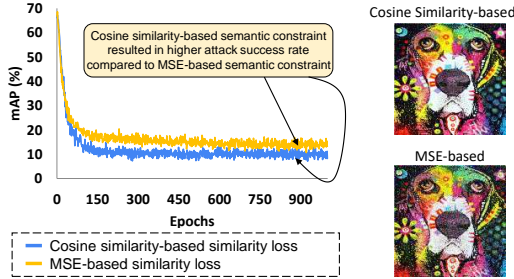


Fig. 5: Impact of different similarity metrics on the effectiveness of the generated patch.

B. Influence of Different Transformations

To evaluate the capacity of our technique to withstand different set of transformations, we incorporate different combinations of transformations in both patch optimization process ours and the GAN-based; With random scaling, with random noise (Brightness, Contrast, and Gaussian Noise) and random scaling, and with random noise (Brightness, Contrast, and Gaussian Noise), random rotation, and random scaling. As shown in Figure 6, our technique outperforms the GAN-based technique and resulted in a higher attack success rate for different transformations, this could be explained by the too limited latent space of the GAN-based technique compared to our technique which provides higher flexibility since it's based on directly manipulating the pixels of the patch.

We run a number of digital experiments on the INRIA dataset to assess the performance influence of the patch size with respect to the size of the target object (person). Table VIII shows that the larger the size of the patch is, the stronger its attack performance as expected.

TABLE VIII: Attack performance of adversarial patches in different size settings for the INRIA dataset.

Patch size	0.1	0.2	0.3
mAP	55.7%	8.81%	5.32%

D. AdvART based on Different Art Work

We also targeted other artistic patterns, we used the cosine similarity-based similarity loss to generate artistic adversarial

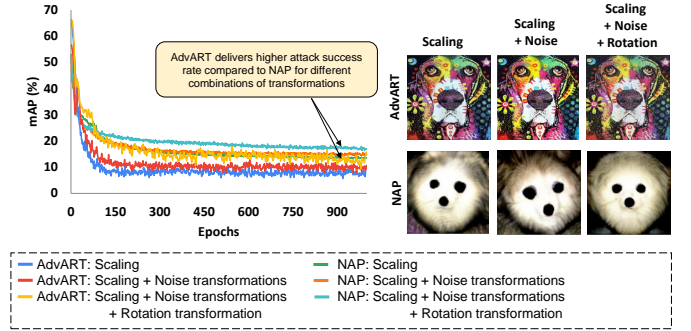


Fig. 6: Mean Average Precision (mAP) convergence curves when training a GAN-based technique (NAP) and our technique (AdvART) with different combinations of transformations.

patches. Our findings revealed that these patches retained a high performance, achieving an average success rate of 90% on the INRIA dataset when using the Yolov4tiny object detector. For instance, when employing patch (a), the mean Average Precision (mAP) dropped significantly, reaching as low as 9.85%.

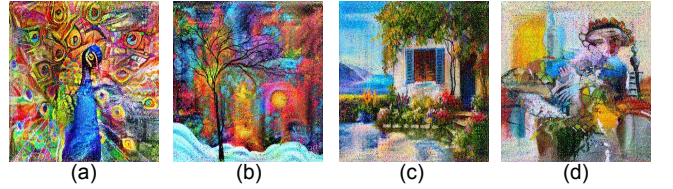


Fig. 7: Illustrations of AdvART based on different art work.

TABLE IX: Attack performance of adversarial patches on different art work in Figure 7 when attacking Yolov4tiny.

Patch	(a)	(b)	(c)	(d)
mAP	9.85%	10.2%	11.33%	15.14%

VIII. CONCLUSION

In this paper, we introduce a novel framework for producing realistic/naturalistic and artistic physical adversarial

patches for object detectors. AdvART is a framework that provides more flexibility in terms of integrated transformations when compared to GAN-based approaches, and it is capable of successfully producing realistic adversarial patches with natural/artistic patterns while retaining competitive attack performance compared to GAN-based techniques and non-naturalistic ones.

REFERENCES

- [1] A. Kurakin *et al.*, “Adversarial examples in the physical world,” *CoRR*, vol. abs/1607.02533, 2016. [Online]. Available: <http://arxiv.org/abs/1607.02533>
- [2] I. Evtimov *et al.*, “Robust physical-world attacks on machine learning models,” *CoRR*, vol. abs/1707.08945, 2017. [Online]. Available: <http://arxiv.org/abs/1707.08945>
- [3] A. Guesmi *et al.*, “Saam: Stealthy adversarial attack on monocular depth estimation,” *arXiv preprint arXiv:2308.03108*, 2023.
- [4] A. Guesmi, M. A. Hanif, I. Alouani, and M. Shafique, “Aparate: Adaptive adversarial patch for cnn-based monocular depth estimation for autonomous navigation,” *arXiv preprint arXiv:2303.01351*, 2023.
- [5] A. Guesmi, M. A. Hanif, B. Ouni, and M. Shafique, “Physical adversarial attacks for camera-based smart systems: Current trends, categorization, applications, research challenges, and future outlook,” *IEEE Access*, 2023.
- [6] K. Eykholt *et al.*, “Physical adversarial examples for object detectors,” in *Proceedings of the 12th USENIX Conference on Offensive Technologies*, ser. WOOT’18. USA: USENIX Association, 2018, p. 1.
- [7] S. Thys *et al.*, “Fooling automated surveillance cameras: adversarial patches to attack person detection,” *CoRR*, vol. abs/1904.08653, 2019. [Online]. Available: <http://arxiv.org/abs/1904.08653>
- [8] Y. Zhao *et al.*, “Seeing isn’t believing: Towards more robust adversarial attack against real world object detectors,” ser. CCS ’19, New York, NY, USA, 2019, p. 1989–2004.
- [9] S. Pavlitskaya *et al.*, “Feasibility of inconspicuous gan-generated adversarial patches against object detection,” 2022. [Online]. Available: <https://arxiv.org/abs/2207.07347>
- [10] T. Bai *et al.*, “Inconspicuous adversarial patches for fooling image-recognition systems on mobile devices,” *IEEE Internet of Things Journal*, vol. 9, no. 12, pp. 9515–9524, 2022.
- [11] Y.-C.-T. Hu *et al.*, “Naturalistic physical adversarial patch for object detectors,” in *2021 IEEE/CVF International Conference on Computer Vision (ICCV)*, 2021, pp. 7828–7837.
- [12] J. Liu *et al.*, “A two-stage generative adversarial networks with semantic content constraints for adversarial example generation,” *IEEE Access*, vol. 8, pp. 205 766–205 777, 2020.
- [13] A. Guesmi *et al.*, “Dap: A dynamic adversarial patch for evading person detectors,” 2023.
- [14] N. Dalal *et al.*, “Histograms of oriented gradients for human detection,” in *2005 IEEE Computer Society Conference on Computer Vision and Pattern Recognition (CVPR’05)*, vol. 1, 2005, pp. 886–893 vol. 1.
- [15] A. Bochkovskiy *et al.*, “Yolov4: Yolov4: Optimal speed and accuracy of object detection,” *arXiv*, 2020.
- [16] J. Redmon *et al.*, “Yolov3: An incremental improvement,” *arXiv*, 2018.
- [17] L. Huang *et al.*, “UPC: learning universal physical camouflage attacks on object detectors,” *CoRR*, vol. abs/1909.04326, 2019.
- [18] M. Lee *et al.*, “On physical adversarial patches for object detection,” *CoRR*, vol. abs/1906.11897, 2019. [Online]. Available: <http://arxiv.org/abs/1906.11897>
- [19] K. Xu, G. Zhang, S. Liu, Q. Fan, M. Sun, H. Chen *et al.*, “Adversarial t-shirt! evading person detectors in a physical world,” in *ECCV*, 2020.
- [20] Z. Wu *et al.*, “Making an invisibility cloak: Real world adversarial attacks on object detectors,” in *ECCV*, 2020.
- [21] A. Voynov and A. Babenko, “Unsupervised discovery of interpretable directions in the gan latent space,” in *International Conference on Machine Learning*. PMLR, 2020, pp. 9786–9796.
- [22] T. Karras *et al.*, “Analyzing and improving the image quality of stylegan,” 2020.
- [23] D. P. Kingma *et al.*, “Adam: A method for stochastic optimization,” 2014. [Online]. Available: <https://arxiv.org/abs/1412.6980>
- [24] J. Redmon, S. K. Divvala, R. B. Girshick, and A. Farhadi, “You only look once: Unified, real-time object detection,” *CoRR*, vol. abs/1506.02640, 2015. [Online]. Available: <http://arxiv.org/abs/1506.02640>
- [25] J. Redmon and A. Farhadi, “YOLO9000: better, faster, stronger,” *CoRR*, vol. abs/1612.08242, 2016. [Online]. Available: <http://arxiv.org/abs/1612.08242>
- [26] A. Athalye *et al.*, “Synthesizing robust adversarial examples,” in *International Conference on Machine Learning*, 2017.
- [27] A. Mahendran *et al.*, “Understanding deep image representations by inverting them,” in *Proceedings of the IEEE conference on computer vision and pattern recognition*, 2015, pp. 5188–5196.
- [28] M. Andriluka *et al.*, “2d human pose estimation: New benchmark and state of the art analysis,” in *IEEE Conference on Computer Vision and Pattern Recognition (CVPR)*, June 2014.
- [29] Z. Wang and A. C. Bovik, “A universal image quality index,” *IEEE signal processing letters*, vol. 9, no. 3, pp. 81–84, 2002.